Heat stress as an emerging constraint on global dairy systems: global gridded CMIP6 projections and national-scale milk loss exposure

Dimitri Defrance, Tiffanie Lescure

December 16, 2025

Preprint – Not peer reviewed

This manuscript is a preprint submitted to *Environmental Research: Food Systems*. It has not yet undergone peer review and should not be cited as a final publication.

The preprint is made available for early dissemination and discussion via **EarthArXiv**.

All results, interpretations and conclusions are those of the authors and may be revised following peer review.

Abstract

Dairy production is a key component of global food systems, providing essential nutrients and supporting rural livelihoods, but it is increasingly exposed to heat stress under climate change. Here, we present a spatially explicit global assessment of heat-stress exposure and potential milk-yield losses using bias-corrected CMIP6 climate projections at 0.25° resolution combined with gridded livestock distribution data.

Daily Temperature–Humidity Index (THI) is computed from maximum air temperature and mean relative humidity using five CMIP6 models at 0.25° resolution. Heat-stress exposure is quantified through exceedance metrics of established physiological thresholds (THI $\geq$ 72 and higher values for sensitivity analysis). Milk-yield losses are estimated using an empirical quadratic loss function and aggregated spatially using FAO Gridded Livestock of the World (GLW3) cattle densities. National-scale losses are calibrated against FAOSTAT milk production, and results are reported for OECD countries using both absolute and per-capita indicators based on a fixed population baseline.

Results show that heat stress is already a structural feature of dairy production in many regions, with recurrent THI exceedances under present-day climate. Future warming leads to a pronounced intensification and seasonal extension of heat stress, particularly in extratropical dairy systems. By the end of the century under SSP5–8.5, projected milk-yield losses become non-marginal for several major dairy producers, while per-capita indicators reveal strong heterogeneity in potential exposure across OECD countries. In tropical regions, THI exceedances exhibit saturation behaviour, whereas mid-latitude systems experience a marked lengthening of the heat-stress season.

By combining climate projections with spatial livestock data and national production statistics, this study provides a consistent framework to translate biophysical heat stress into food-system-relevant exposure metrics. While not accounting for adaptation or structural change, the results highlight heat stress as an emerging systemic constraint on dairy productivity and provide a quantitative baseline for evaluating future adaptation strategies and food-system resilience.

1 Introduction

Milk and dairy products play a central role in global food systems, providing high-quality protein, essential micronutrients, and a major source of income for rural households worldwide. In 2022, global milk production exceeded 930 million tonnes, with bovine milk accounting for more than 80% of total output [1]. Beyond its contribution to caloric intake, milk is a nutrient-dense food that supplies calcium, vitamin B_{12}, riboflavin and high-quality amino acids, making it particularly important for child growth, maternal health and dietary quality [2–4]. As such, dairy production constitutes a key pillar of food and nutrition security in many regions of the world.

The economic and structural importance of dairy systems is well documented in global assessments such as the OECD–FAO Agricultural Outlook and the

IFCN Dairy Report, which highlight the role of milk in income generation, trade flows and agri-food value chains [5, 6]. Demand for dairy products is projected to continue increasing over the coming decades, driven by population growth, urbanisation and dietary transitions, particularly in emerging economies [5, 7]. At the same time, dairy systems are increasingly scrutinised for their environmental footprint and land-use requirements, placing productivity and efficiency at the centre of sustainability debates [8]. Sustaining milk production under changing climatic conditions therefore represents a critical challenge for food systems, rural livelihoods and agricultural resilience.

Among climate-related pressures affecting livestock systems, heat stress has emerged as one of the most direct and damaging threats to dairy production. Elevated temperature and humidity reduce feed intake, milk synthesis, reproductive performance and immune function, leading to measurable declines in milk yield and animal welfare [9–11]. High-producing dairy cows are particularly vulnerable due to their high metabolic heat load and limited capacity for heat dissipation [12, 13]. With rising global temperatures and increasing frequency and intensity of heat extremes, heat stress is expected to become an increasingly dominant constraint on dairy productivity [14, 15].

The Temperature–Humidity Index (THI) is the most widely used indicator of thermal stress in dairy cattle, combining air temperature and relative humidity into a physiologically meaningful metric. A commonly applied formulation based on daily maximum temperature and mean relative humidity was proposed by St-Pierre et al. [12]. Numerous empirical studies have shown that milk yield declines significantly when THI exceeds 72, with losses increasing nonlinearly at higher stress levels [10, 16]. THI-based loss functions have been applied across a range of production systems and climatic contexts, including the United States [16], Europe [17] and East Asia [18]. While these studies consistently highlight substantial vulnerability of dairy systems to heat stress, they remain geographically limited and often rely on heterogeneous data and methodologies.

Despite a growing body of regional evidence, there is still a lack of high-resolution, globally consistent assessments of future heat-stress exposure and associated milk-yield losses. Many existing analyses rely on station observations or coarse-resolution climate models, limiting their ability to resolve spatial heterogeneity in exposure and vulnerability. Moreover, relatively few studies explicitly integrate climate projections with spatial livestock distributions to estimate potential national-scale production losses in a harmonised global framework [19, 20]. This gap limits the comparability of results across countries and constrains the translation of climate signals into decision-relevant indicators.

Recent advances in climate modelling and data availability now make such assessments feasible. The Coupled Model Intercomparison Project Phase 6 (CMIP6) provides a comprehensive multi-model framework for analysing future climate change under shared socio-economic pathways [21]. Bias-corrected daily climate projections are available through the NASA NEX-GDDP-CMIP6 dataset at 0.25° spatial resolution [22], and are widely used in climate-impact assessments. These projections are commonly evaluated against the ERA5 reanalysis, which offers a physically consistent, observation-constrained represen-

tation of recent climate conditions [23]. In parallel, high-resolution livestock density datasets such as FAO's Gridded Livestock of the World v3 (GLW3) enable the spatial localisation of climate impacts on dairy systems [24].

In this study, we provide a global assessment of future heat-stress risks to dairy cattle using five bias-corrected CMIP6 models from the NEX-GDDP-CMIP6 archive. We compute daily THI, derive exceedance-based heat-stress indicators (THI $\geq$ 72 and THI $\geq$ 77), and estimate milk-yield losses using an empirical quadratic loss function. Losses are aggregated spatially using GLW3 dairy cattle density and scaled with FAOSTAT production statistics to estimate potential national-scale impacts. We analyse three climate scenarios (SSP1–2.6, SSP2–4.5 and SSP5–8.5) across baseline (1991–2020), mid-century (2041–2070) and end-century (2071–2100) periods.

To our knowledge, this is the first global-scale, multi-model assessment that combines CMIP6 projections at 0.25° resolution, validated THI thresholds, empirical milk-loss functions and spatial livestock distributions to quantify both heat-stress exposure and potential national-scale milk production losses. By resolving subnational gradients in thermal stress and explicitly linking them to dairy cattle density and national production statistics, this study highlights strong scenario dependence, pronounced regional inequalities and the emergence of thermally critical environments for dairy production. These results provide a quantitative basis for anticipating future pressures on dairy systems and for informing adaptation strategies, herd management and long-term planning.

2 Materials and Methods

2.1 Workflow overview

Figure 1 summarises the analytical steps. Daily maximum temperature (T_{max}) and relative humidity (RH) from bias-adjusted CMIP6 simulations (NEX-GDDP-CMIP6) are used to compute the daily Temperature–Humidity Index (THI). Exceedances above selected thresholds (THI $\geq$ 72, with additional thresholds for sensitivity analyses) are derived at 0.25° resolution.

Daily milk-yield losses are estimated using the St-Pierre quadratic function, producing annual loss per cow (kg cow^{-1} yr^{-1}). A two-step livestock mask is applied: (i) countries where bovine milk represents less than 85% of total milk production (FAOSTAT, 2010–2014 mean) are excluded; (ii) within retained countries, grid cells with fewer than 20 cattle per 0.25° pixel (GLW3, aggregated) are removed to avoid artefacts and mixed-ruminant systems.

Pixel-level losses are aggregated to the national scale using GLW3 cattle numbers. For OECD countries, we compute two final exposure metrics: (i) annual present-day losses (tonnes yr^{-1}), and (ii) future losses per inhabitant (kg cap^{-1} yr^{-1}) using a fixed 2010–2014 population baseline.

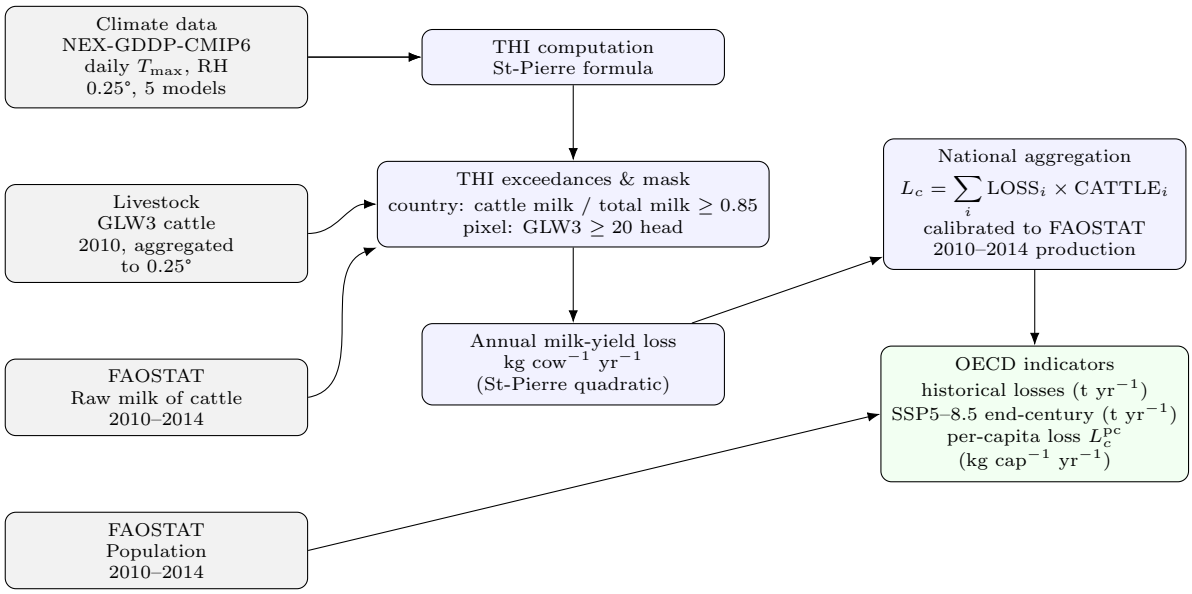

Figure 1: Schematic workflow of the dairy heat-stress assessment. Daily maximum temperature and relative humidity from NEX-GDDP-CMIP6 are converted to THI, from which exceedance metrics and annual milk-yield loss per cow are derived. A two-step livestock mask, based on GLW3 cattle densities and FAOSTAT milk-type ratios, restricts the analysis to dairy-dominated systems. Pixel-level losses are aggregated to OECD countries using gridded cattle numbers and calibrated to 2010–2014 FAOSTAT production, yielding national and per-capita loss indicators.

2.2 Climate and livestock data

We use the NASA NEX-GDDP-CMIP6 dataset [22], which provides bias-corrected daily maximum temperature and near-surface relative humidity at 0.25° resolution. Data will be compare to ERA5 in terms of THI. Five models with complete RH fields are analysed: GFDL-ESM4, IPSL-CM6A-LR, MPI-ESM1-2-HR, MRI-ESM2-0 and UKESM1-0-LL. We evaluate one historical baseline (1995–2014) and three future scenarios: SSP1–2.6, SSP2–4.5 and SSP5–8.5 for mid-century (2041–2070) and end-century (2071–2100).

Cattle densities are obtained from the Gridded Livestock of the World v3 dataset (GLW3) [24]. We use the 2010 cattle layer (all cattle: dairy + beef) and aggregate it to 0.25° using mean-preserving averaging. National milk production and population data are taken from FAOSTAT (item "Raw milk of cattle", flags A/E), averaged over 2010–2014. These fixed baselines ensure that demographic or structural agricultural changes do not influence the climate-impact signal.

2.3 THI computation

Daily heat stress is quantified using the St-Pierre temperature–humidity index formulation:

$$\mathrm{THI}_{\max} = (1.8T_{\max} + 32)\,(0.55 - 0.0055\,RH)\,(1.8T_{\max} - 26), \tag{1}$$

where $T_{\max}$ is daily maximum temperature (°C) and RH is daily mean relative humidity (%). Maximum temperature is used because it better captures short-term physiological stress in dairy cattle.

We focus on exceedances of THI $\geq$ 72, a widely used threshold for onset of heat-related milk-yield losses in high-yielding temperate breeds. THI $\geq$ 77 denotes severe stress. Additional thresholds (68, 77 and 82) are included in a sensitivity analysis, the latter being relevant for heat-adapted tropical breeds. Exceedance metrics include (i) annual number of days above the threshold and (ii) the mean seasonal cycle of THI $\geq$ 72.

2.4 Milk-yield loss estimation

Milk-yield losses are computed using the quadratic St-Pierre function:

$$\mathrm{LOSS}_{\mathrm{daily}} = 0.0695\,(\mathrm{THI}_{\max} - 72)^2\,1[\mathrm{THI}_{\max} > 72], \tag{2}$$

expressed in kg cow^{-1} day^{-1}. Daily losses are summed to annual totals for each model, scenario and grid cell. The function is calibrated for Holstein cows in temperate intensive systems; losses in tropical regions therefore represent upper-bound estimates rather than breed-specific predictions.

2.5 Livestock mask

A two-step mask is applied to ensure that THI-derived losses are interpreted only for dairy-relevant systems:

1. **National milk-type filter:** Countries are retained only if

$$\frac{\text{Raw milk of cattle}}{\text{Total milk}} \geq 0.85,$$

   using FAOSTAT 2010–2014 means (flags A/E). This excludes regions where buffalo, goats or mixed ruminants dominate milk production.

2. **Local dairy-density filter:** Within retained countries, 0.25° grid cells are kept only if aggregated GLW3 density exceeds 20 cattle per cell. This ensures that pixel-level results reflect meaningful dairy production systems.

This full mask is applied to all spatial LOSS maps. For national aggregation, all GLW3 cattle within retained countries are used (i.e., without applying the 20 threshold) to avoid underestimating extensive systems.

2.6 National aggregation and per-capita indicator

Annual pixel-level losses (kg cow^{-1} yr^{-1}) are multiplied by GLW3 cattle counts and summed across each country:

$$L_c = \sum_{i \in c} \mathrm{LOSS}_i \times \mathrm{CATTLE}_i.$$

Totals are calibrated to FAOSTAT 2010–2014 milk production to ensure consistency between gridded cattle counts and national statistics. We restrict reporting to OECD countries that satisfy the national milk-type filter.

To express losses relative to population exposure, we compute an annual per-capita metric:

$$L_c^{\mathrm{pc}} = \frac{L_c}{P_c},$$

where P_c is the FAOSTAT 2010–2014 average national population. This indicator expresses the climatic pressure on dairy availability under constant demographic conditions.

3 Validation

Overall, the ensemble reproduces the large-scale latitudinal gradients observed in ERA5. Differences are spatially structured and concentrate in (i) arid and semi-arid regions, (ii) complex topography, and (iii) coastal and lake-influenced grid cells, consistent with the strong sensitivity of threshold-based indicators to humidity fields and land–surface representation. In most dairy-relevant mid-latitude regions, differences are typically on the order of a few tens of days per year, but can locally exceed this range near sharp climatic and surface-type transitions. Given that the milk-loss function is nonlinear and activated only above THI ≥ 72, local discrepancies in exceedance counts below this threshold have limited influence on aggregated milk-yield loss estimates.

Importantly, subsequent impact estimates further restrict the domain of interpretation. Milk-yield loss maps are computed only within the two-step livestock mask (countries dominated by bovine milk production and grid cells with meaningful dairy-cattle presence), thereby excluding large fractions of deserts, sparsely grazed regions and mixed-milk systems where exceedance-based discrepancies are most pronounced. Country-scale production losses are then reported only for OECD members, which concentrates the analysis on temperate and subtropical production basins where both ERA5 and the ensemble show coherent spatial gradients. Together, these successive filters ensure that the loss and production metrics are derived from the subset of regions where the THI signal is both relevant to dairy systems and most robustly comparable across datasets.

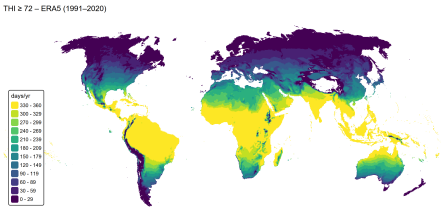

(a) THI $\geq$ 72 – ERA5 (1991–2020)

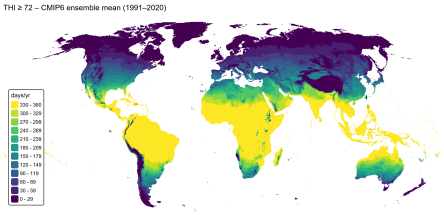

(b) THI $\geq$ 72 – CMIP6 ensemble mean (1991–2020)

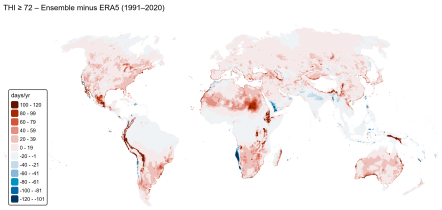

(c) THI $\geq$ 72 – CMIP6 ensemble minus ERA5 (1991–2020)

Figure 2: Comparison of heat stress (THI $\geq$ 72) between ERA5 (1991–2020) and CMIP6 ensemble mean. The bottom panel shows the difference between the two (Ensemble minus ERA5). Results confirm the robustness of the ensemble mean and highlight discrepancies in projected heat stress levels.

4 Results

4.1 Annual exceedances of THI $\geq$ 72

We first analyse the annual number of days exceeding the primary heat-stress threshold used in this study, THI $\geq$ 72, which marks the onset of heat-related milk-yield losses in high-producing dairy systems. Figure 3 presents the spatial distribution of THI $\geq$ 72 exceedances for the ensemble mean of five CMIP6 models, for the baseline (1991–2020), mid-century (2041–2070) and end-century (2071–2100) periods under SSP2–4.5 and SSP5–8.5 (see Figure S 1 in supplementary information for SSP1–2.6).

During the baseline period, tropical and equatorial regions already experience very frequent exceedances, commonly exceeding 250–300 days yr^{-1}, indicating quasi-permanent heat-stress conditions. Subtropical regions, including large parts of South Asia, the Middle East and northern Africa, typically exhibit 100–200 days yr^{-1}. In contrast, temperate regions such as Europe, North America and East Asia show substantially lower exposure, generally below 30–

60 days yr^{-1}, with exceedances largely confined to the warm season.

Future projections indicate a pronounced regional intensification, with a strong dependence on emission scenario. Under SSP5–8.5, THI $\geq$ 72 exceedances expand markedly into mid-latitude regions by the end of the century. Large areas of Europe and North America reach 80–150 days yr^{-1}, while parts of southern Europe, the central United States and eastern China approach or exceed 100 days yr^{-1}. Under SSP2–4.5, increases are more moderate but remain widespread, particularly across regions that currently experience episodic heat stress.

In equatorial regions, projected changes are smaller in relative terms, reflecting a saturation effect whereby THI $\geq$ 72 conditions are already present during most of the year in the baseline climate. In these areas, future warming primarily reinforces the persistence and intensity of heat stress rather than substantially increasing the number of exceedance days. Despite differences in absolute magnitudes across individual models, the ensemble mean consistently reproduces the main spatial gradients, regional hotspots and scenario contrasts. Individual-model results are shown in Supplementary Figure S 2 and confirm the robustness of these patterns across the CMIP6 ensemble. This spatial contrast between saturation-dominated and seasonally varying regions motivates a closer examination of the seasonal cycle of THI exceedances in the following section.

4.2 Seasonal cycle and monthly exceedance (THI $\geq$ 72)

To assess changes in the timing and persistence of heat stress, we analyse the mean monthly number of days with THI $\geq$ 72, shown as ensemble means for the baseline (1991–2020), SSP2–4.5 and SSP5–8.5 end-century periods (Figure 4). Results are presented separately for the Northern Hemisphere mid-latitudes (HM, 30°N–60°N), the tropics (30°S–30°N), and the Southern Hemisphere mid-latitudes (HS, 60°S–30°S).

In the Northern Hemisphere mid-latitudes (Figure 4a), baseline exceedances are strongly seasonal, with fewer than 5 days $month^{-1}$ in winter and a pronounced summer peak reaching 20–22 days $month^{-1}$ in July–August. Under future scenarios, the heat-stress season both intensifies and expands. SSP2–4.5 leads to earlier spring onset and delayed autumn decline, while SSP5–8.5 further amplifies summer peaks to around 25–28 days $month^{-1}$ and substantially increases exceedances in May, June and September. This indicates a lengthening of the heat-stress season rather than a simple amplification of the summer maximum.

In the equatorial regions (Figure 4b), THI $\geq$ 72 exceedances occur throughout the year, with limited seasonal variability. Baseline values typically range between 23 and 28 days $month^{-1}$, already close to saturation. Future warming results in only modest absolute increases, mainly by pushing several months closer to the upper bound of 30 days $month^{-1}$. This behaviour reflects a saturation regime in which heat stress is already persistent year-round, and climate change primarily increases the continuity and intensity of exposure rather than

altering its seasonal structure. It should be noted that, in many tropical regions, dairy systems rely on heat-adapted breeds for which the physiological response to a given THI threshold may differ from that of high-producing temperate cattle.

In the Southern Hemisphere mid-latitudes (Figure 4c), a clear seasonal cycle is also evident, with baseline peaks during austral summer (December–February) reaching around 18–22 days month^{-1} and near-zero exceedances during winter months. Future scenarios mirror the Northern Hemisphere response, with enhanced summer peaks and a broadening of the heat-stress season into the shoulder months. Under SSP5–8.5, exceedances during austral summer approach 23–26 days month^{-1}, while spring and autumn months experience a marked increase compared to the baseline.

Overall, the monthly analysis highlights two distinct regimes: a saturation-dominated tropical regime with quasi-permanent heat stress, and a seasonality-dominated extratropical regime where climate change primarily acts to extend the duration and intensity of the heat-stress season. These seasonal shifts provide essential context for interpreting annual exceedance metrics and for understanding the timing of potential impacts on dairy production. In this context, the choice of a single THI threshold may influence the apparent magnitude of exposure across regions, motivating a sensitivity analysis to alternative threshold values.

4.3 Sensitivity to alternative thresholds (THI $\geq$ 68, $\geq$ 77 and $\geq$ 82)

We assess the sensitivity of heat-stress exposure to alternative THI thresholds by repeating the exceedance analysis using thresholds of 68, 77 and 82 (Figure 5). These values span a range from mild heat stress (THI $\geq$ 68), commonly associated with early physiological responses, to severe and potentially critical conditions (THI $\geq$ 77 and THI $\geq$ 82), which are increasingly linked to acute production losses and animal welfare risks. Across the ensemble, the main geographical contrasts and scenario-driven patterns remain consistent, indicating that the spatial structure of heat-stress exposure is robust to reasonable variations in threshold choice.

Lowering the threshold to THI $\geq$ 68 substantially increases the spatial extent and duration of exposure, particularly in temperate regions where exceedances are episodic under present-day climate (Figure 5, top row). In contrast, raising the threshold to THI $\geq$ 77 and THI $\geq$ 82 markedly reduces exceedance frequency but preserves the location of major hotspots, notably in tropical and subtropical regions (Figure 5, middle and bottom rows). These higher thresholds therefore isolate areas transitioning from intermittent to severe or quasi-chronic heat-stress conditions, even when annual exceedance counts remain limited.

Detailed sensitivity maps are provided in Supplementary Figure S3, including results for SSP1–2.6 and SSP2–4.5. These supplementary analyses confirm that, despite differences in absolute exceedance frequency, the relative ranking of regions and the contrast between scenarios remain qualitatively unchanged.

Taken together, this sensitivity analysis supports the use of THI $\geq$ 72 as a balanced threshold for subsequent impact assessment, capturing both the emergence of heat stress in temperate regions and its intensification in already warm climates, and providing a consistent basis for estimating milk-yield losses in the following section.

4.4 Milk yield loss per cow

Annual milk-yield losses per cow (kg cow^{-1} yr^{-1}) are estimated by applying the quadratic St-Pierre loss function to all days with THI $\geq$ 72 and aggregating daily losses over each year. Figure 6 shows the ensemble-mean spatial distribution of annual losses per cow for the baseline period (1991–2020), as well as mid-century (2041–2070) and end-century (2071–2100) projections under SSP2–4.5 and SSP5–8.5. Results are shown only for regions retained by the livestock mask, ensuring that losses are displayed for dairy-dominated production systems (For the mask see Figure S4).

In the baseline climate, losses remain generally low in temperate regions, typically below 50–100 kg cow^{-1} yr^{-1}, while higher values are already apparent in subtropical regions characterised by frequent THI exceedances. By mid-century, projected losses increase markedly under both scenarios, with clear spatial contrasts emerging between moderately affected temperate regions and strongly affected subtropical zones. Under SSP5–8.5, end-century losses intensify further, with large areas of southern Europe, the southern United States, parts of South America and eastern China exceeding 200–300 kg cow^{-1} yr^{-1}.

The spatial patterns of milk-yield loss closely mirror those of THI exceedance frequency, confirming that regions experiencing strong increases in the duration and persistence of heat stress also exhibit the largest projected production impacts. Differences between SSP2–4.5 and SSP5–8.5 are modest at mid-century but become pronounced by the end of the century, highlighting the increasing divergence between mitigation pathways in terms of dairy heat-stress impacts.

Although individual models differ in the absolute magnitude of projected losses, they consistently reproduce similar spatial gradients, hotspot locations and scenario contrasts. The full range of inter-model variability (minimum–maximum) is shown in Supplementary Figure S5 Figure S6 , indicating that ensemble-mean patterns provide a robust representation of climate-driven milk-yield loss per cow.

While these maps quantify climate-driven milk-yield losses at the individual cow level, translating such impacts into socio-economic relevance requires accounting for the spatial distribution of cattle and aggregating losses at the national scale. In the following section, we therefore combine pixel-level yield losses with gridded cattle densities to estimate country-level milk production losses, with a specific focus on OECD countries.

4.5 Country-level milk production losses

Pixel-level milk-yield losses are combined with gridded dairy cattle densities from GLW3 to estimate national-scale milk production losses. For each grid cell, annual losses per cow are multiplied by the corresponding number of cattle and aggregated spatially. National totals are subsequently calibrated using FAOSTAT baseline milk production averaged over 2010–2014, ensuring consistency between gridded livestock distributions and reported national statistics.

Table 1 summarises ensemble-mean milk production losses for OECD countries, expressed both in absolute terms (Mt yr^{-1}) and on a per-capita basis (kg yr^{-1} $inhab^{-1}$), for the baseline period and for end-century conditions under SSP5–8.5. Absolute losses vary widely across countries and are primarily driven by the size of national dairy herds combined with the intensity of projected heat stress. Major dairy producers such as the United States, Mexico and Australia exhibit the largest absolute losses, reflecting their substantial cattle numbers and production volumes.

To facilitate comparison across countries with different population sizes, losses are also expressed on a per-capita basis using a fixed population baseline averaged over 2010–2014. This indicator represents the hypothetical redistribution of national production losses across the current population and should therefore be interpreted as an exposure or pressure metric rather than a realised dietary impact. High per-capita losses observed in countries such as Australia, New Zealand and Ireland result from the combination of substantial dairy production and relatively small populations, whereas countries with large populations tend to exhibit lower per-capita values despite high absolute production losses.

These per-capita indicators do not account for future demographic change, international trade, adaptive responses in dairy systems or shifts in consumption patterns, and should not be interpreted as projections of actual milk availability at the individual level. Instead, together with absolute loss estimates, they highlight how climatic stress on dairy production interacts with national production scale, cattle density and population size, revealing strong heterogeneity in potential vulnerability across OECD countries.

5 Discussion

5.1 Key findings: structural exposure and non-marginal losses

This study demonstrates that dairy systems across OECD countries are already structurally exposed to heat stress under present-day climate conditions. Recurrent exceedances of THI ≥ 72 are observed over substantial dairy-producing areas, confirming that thermal stress is no longer an episodic hazard but an emerging structural constraint for intensive dairy systems. Comparable levels of baseline exposure have been documented in regional studies for Europe

and North America [10, 16, 17], but our results extend these findings to a harmonised, multi-country framework.

When cow-level losses are aggregated using gridded cattle densities and calibrated against FAOSTAT production, projected end-century impacts under SSP5–8.5 reach non-marginal levels for several major producers. Absolute losses become substantial for large dairy economies such as the United States, Mexico and Australia, while per-capita losses highlight strong contrasts among OECD countries with smaller populations but highly specialised dairy sectors. Together, these results indicate that heat stress already represents a systemic pressure on dairy productivity, rather than a marginal or future-only risk, consistent with broader assessments of climate impacts on food systems [15].

Beyond magnitude, the seasonal analysis shows that climate change affects dairy systems not only by increasing peak summer stress, but also by extending the duration of the heat-stress season. This lengthening of exposure windows is particularly relevant for cumulative physiological stress, fertility impairment and management burden in dairy cattle [13, 25]. Such effects reinforce the interpretation of heat stress as a chronic constraint under warming conditions.

5.2 Positioning within the existing literature

The negative impacts of heat stress on dairy cattle performance are well established through experimental, observational and economic studies [10–12]. Under climate change, an expanding literature has quantified increasing exposure and productivity risks at regional scales, notably in North America [16], Europe [17] and East Asia [18]. These studies consistently identify THI $\geq$ 72 as a critical threshold for yield decline, but they remain geographically bounded or methodologically heterogeneous.

Our findings are consistent with this literature while extending it in several important ways. By using bias-corrected CMIP6 projections and a harmonised livestock distribution, we provide a spatially explicit, multi-model assessment that preserves subnational gradients and enables cross-country comparison. In addition, by expressing losses in physically interpretable units and normalising them by population, we complement production-focused analyses without conflating climate-driven physiological stress with broader socio-economic drivers such as policy, market dynamics or technological change [15, 20].

5.3 Seasonality versus saturation regimes

The results reveal two distinct climatic regimes that shape the interpretation of THI-based indicators. In tropical and equatorial regions, THI $\geq$ 72 conditions are already frequent in the baseline climate, leading to near-saturation of exceedance counts close to the theoretical maximum of 30 days month^{-1}. Similar saturation behaviour has been reported in previous assessments of heat stress in warm and humid regions [10, 14]. In these environments, future warming primarily reinforces the persistence and intensity of heat stress rather than substantially increasing exceedance frequency.

In contrast, extratropical regions (including most OECD dairy systems) remain strongly seasonal. There, climate change acts by both intensifying peak summer stress and extending the heat-stress season into spring and autumn. Extended exposure reduces opportunities for physiological recovery and has been shown to exacerbate cumulative impacts on milk yield, reproduction and animal welfare [13, 25]. The sensitivity analysis confirms that these spatial and seasonal contrasts are robust to reasonable variations in THI threshold choice.

5.4 From cow-level losses to national-scale pressure

A key contribution of this study is the translation of per-cow yield losses into national-scale production losses calibrated to FAOSTAT baselines. This step bridges physiological indicators and policy-relevant metrics. Previous studies have either focused on animal-level responses [12] or reported aggregated impacts without explicit spatial weighting [14]. By combining THI-derived losses with gridded cattle densities, we capture the joint influence of climatic exposure and production concentration.

Expressing losses on a per-capita basis further highlights how similar climatic signals can translate into markedly different national pressures depending on population size and production specialisation. As noted in earlier work on climate impacts and food systems, demographic context strongly modulates vulnerability even when biophysical hazards are comparable [15, 20]. In this study, per-capita losses are therefore interpreted as exposure indicators rather than projections of realised dietary outcomes.

5.5 Uncertainties and limitations

Several limitations must be acknowledged. First, THI is computed from daily maximum temperature and mean relative humidity and does not explicitly represent night-time cooling, multi-day heatwave duration or radiative and wind effects, which can influence recovery and cumulative stress [25]. Second, the milk-loss function is calibrated for high-producing dairy systems and does not account for breed differences, acclimation or genotype-by-environment interactions [13, 26]. Third, adaptive management practices such as cooling, housing design or dietary adjustments are not explicitly represented [11, 27]. Finally, the spatial distribution of dairy cattle is assumed to be stationary, whereas long-term climate pressure may induce relocation or structural transformation of production systems.

These limitations primarily affect the magnitude of projected losses rather than their spatial structure or scenario dependence. The consistency of patterns across climate models and sensitivity thresholds supports the robustness of the qualitative conclusions.

5.6 Implications for adaptation and future work

The projected intensification and seasonal extension of heat stress imply that adaptation will become increasingly central for sustaining dairy productivity in OECD countries. Technological measures (cooling systems, housing design), management adjustments and genetic selection for thermotolerance have all been identified as effective but potentially costly responses [11, 14, 27]. By isolating the climatic component of heat stress using a consistent multi-model framework, this study provides a baseline against which the potential benefits and limits of such adaptation strategies can be evaluated.

Future research should integrate cumulative heat-load metrics, explicitly represent adaptation pathways, and link biophysical losses to economic and welfare outcomes. Validation against reanalysis-based THI climatologies and observed seasonal cycles will further strengthen confidence in baseline exposure estimates and improve attribution of future changes.

6 Conclusion

This study provides a spatially explicit assessment of heat-stress impacts on dairy production based on bias-corrected CMIP6 climate projections, established THI thresholds and an empirical milk-yield loss function. By combining daily climate indicators with gridded livestock distributions and national production statistics, we quantify how climate warming modifies both the intensity and the seasonal structure of thermal stress affecting dairy systems.

Our results show that heat stress is already a structural feature of dairy production across many OECD regions and is projected to intensify further under future warming. In extratropical systems, climate change acts primarily by extending the duration of the heat-stress season, while in warmer regions it reinforces persistent exposure regimes. When translated from cow-level responses to national-scale production metrics, these changes lead to non-marginal milk production losses by the end of the century, with strong heterogeneity across countries driven by differences in climate exposure, cattle density and population size.

The framework developed here demonstrates how climate projections can be operationalised into decision-relevant indicators without conflating biophysical stress with socio-economic drivers of production. While uncertainties remain—related to breed diversity, management practices, adaptation measures and the simplified representation of heat stress—the consistency of spatial patterns and scenario contrasts across the multi-model ensemble supports the robustness of the main conclusions.

Overall, this work highlights heat stress as an emerging structural constraint on dairy productivity in industrialised systems and provides a quantitative baseline for evaluating adaptation strategies. As warming continues, effective mitigation and adaptation will be essential to sustain dairy production and to manage the increasing climatic pressure on livestock systems.

The author thanks the developers and data providers of the CMIP6 models, the NASA NEX-GDDP data archive, the FAO Gridded Livestock of the World (GLW3) dataset, and FAOSTAT for making their datasets publicly available. All computations were carried out using open-source software on the author's own computing resources. This research received no external funding.

Conceptualization: D.D. & T.L. **Methodology:** D.D. & T.L. **Software:** D.D. **Formal analysis:** D.D. **Data curation:** D.D. **Validation:** D.D. **Visualization:** D.D. **Writing – original draft:** D.D. **Writing – review & editing:** D.D. & T.L.

All data used in this study are publicly available. Bias-corrected CMIP6 climate projections were obtained from NASA NEX-GDDP. Dairy cattle distribution data (GLW3) were obtained from FAO (https://data.apps.fao.org). National milk production statistics were retrieved from FAOSTAT (https://www.fao.org/faostat). Processed indicators and scripts used to generate the results will be made available in a public repository upon publication (Zenodo and GitHub).

References

[1] FAO 2023 FAOSTAT: Raw Milk of Cattle Production `https://www.fao.org/faostat/` food and Agriculture Organization of the United Nations, Rome

[2] Murphy S P and Allen L H 2003 *The Journal of Nutrition* **133** 3932S–3935S

[3] Dror D K and Allen L H 2011 *Food and Nutrition Bulletin* **32** 227–243

[4] Beal T and Ortenzi F 2022 *Frontiers in Nutrition* **9** 806566

[5] OECD and FAO 2025 Oecd-fao agricultural outlook 2025–2034: Dairy and dairy products chapter

[6] Hemme T and Otte J 2021 *IFCN Dairy Report 2021* (IFCN)

[7] Gerosa S and Skoet J 2012 Milk availability: Trends in production and demand and medium-term outlook Tech. rep. FAO ESA

[8] Wirsenius S, Azar C and Berndes G 2010 *Agricultural Systems* **103** 621–638 model-based scenarios of global agricultural land use under different dietary and livestock productivity assumptions.

[9] Silanikove N 2000 *Journal of Dairy Science* **83** 217–232

[10] West J W 2003 *Journal of Dairy Science* **86** 2131–2144

[11] Polsky L and von Keyserlingk M 2017 *Journal of Dairy Science* **100** 8645–8657

[12] St-Pierre N, Cobanov B and Schnitkey G 2003 *Journal of Dairy Science* **86** E52–E77

[13] Bernabucci U, Biffani S, Buggiotti L, Vitali A, Lacetera N and Nardone A 2010 *Journal of Dairy Science* **93** 577–579

[14] Nardone A, Ronchi B, Lacetera N, Ranieri M and Bernabucci U 2006 *Livestock Science* **103** 173–181

[15] Pörtner H O, Roberts D, Adams H *et al.* (eds) 2022 *Climate Change 2022: Impacts, Adaptation and Vulnerability* (Cambridge University Press)

[16] Key N and Sneeringer S 2014 *American Journal of Agricultural Economics* **96** 1136–1156

[17] Mauger G, Bauman Y, Nennich T and Salathé E 2015 *The Professional Geographer* **67** 121–131

[18] Jeon H and Kim J 2023 *Animals* **13** 215

[19] Herrero M, Havlík P, Valin H *et al.* 2013 *Proceedings of the National Academy of Sciences* **110** 20888–20893

[20] Thornton P K and Herrero M 2015 *Global Food Security* **7** 95–102

[21] Eyring V, Bony S, Meehl G *et al. Geoscientific Model Development* **9**

[22] Thrasher B, Wang W, Michaelis A, Melton J R, Lee H and Bond-Lamberty B 2022 *Scientific Data* **9** 262

[23] Hersbach H, Bell B, Berrisford P *et al.* 2020 *Quarterly Journal of the Royal Meteorological Society* **146** 1999–2049

[24] FAO 2020 Available at: `https://www.fao.org/livestock-systems/global-distributions`

[25] Lacetera N, Bernabucci U, Ronchi B and Nardone A 2009 *Livestock Science* **130** 57–69

[26] Ravagnolo O and Misztal I 2000 *Journal of Dairy Science* **83** 2120–2125

[27] Hristov A N, Oh J, Firkins J L *et al.* 2018 *Journal of Dairy Science* **101** 372–418

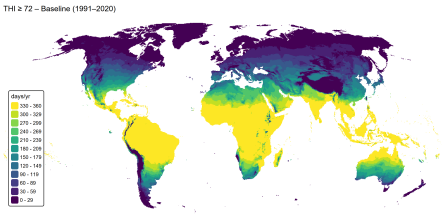

(a) Baseline (1991–2020)

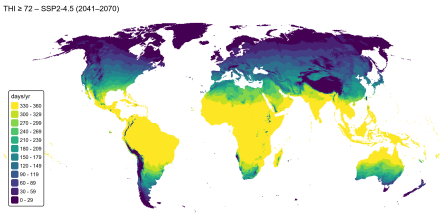

(b) SSP2–4.5 (2041–2070)

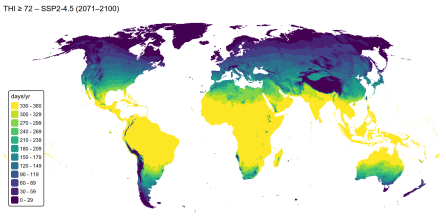

(c) SSP2–4.5 (2071–2100)

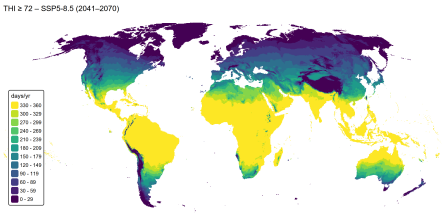

(d) SSP5–8.5 (2041–2070)

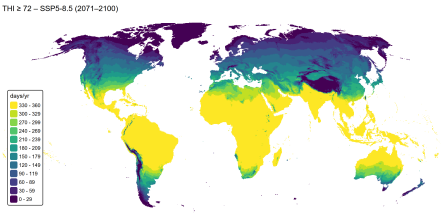

(e) SSP5–8.5 (2071–2100)

Figure 3: Annual number of days with THI $\geq$ 72 for the ensemble mean: baseline (1991–2020, top left) and mid- and end-century projections under SSP2–4.5 (top row) and SSP5–8.5 (bottom row).

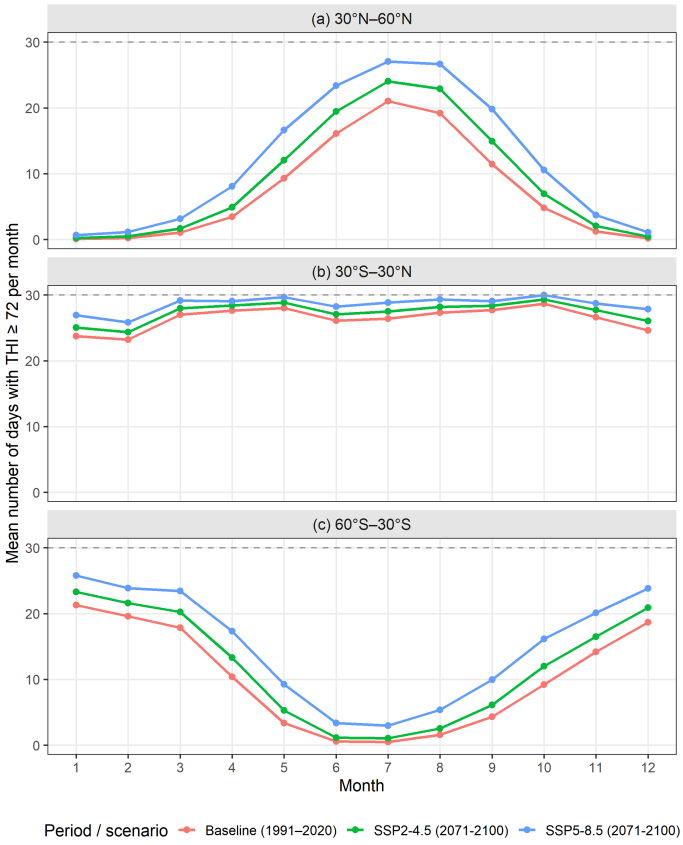

Figure 4: Seasonal cycle of the area-weighted mean number of days per month with THI ≥ 72 for three latitude bands: (a) 30°N–60°N, (b) 30°S–30°N and (c) 60°S–30°S. Coloured lines show the baseline climate (1991–2020), mid-century under SSP2-4.5 (2041–2070) and end-century under SSP5-8.5 (2071–2100). The dashed horizontal line at 30 days month^{-1} indicates the upper bound corresponding to daily exceedance throughout the month.

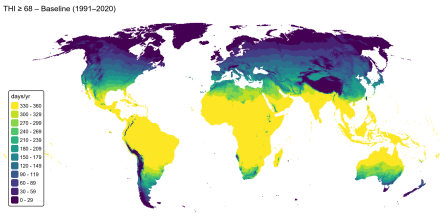

(a) THI $\geq$ 68 – Baseline (1991–2020)

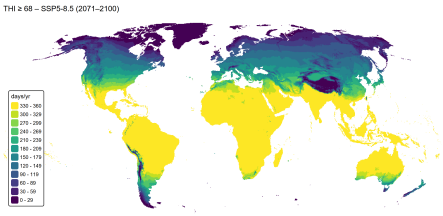

(b) THI $\geq$ 68 – SSP5–8.5 (2071–2100)

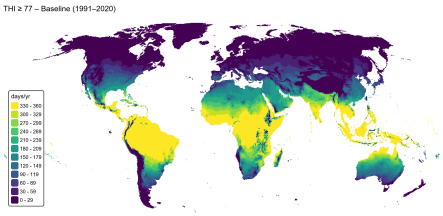

(c) THI $\geq$ 77 – Baseline

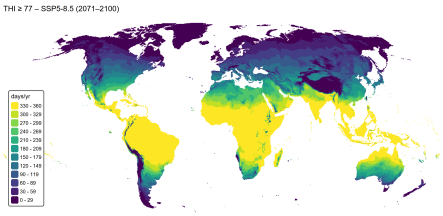

(d) THI $\geq$ 77 – SSP5–8.5

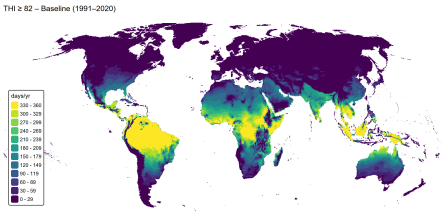

(e) THI $\geq$ 82 – Baseline

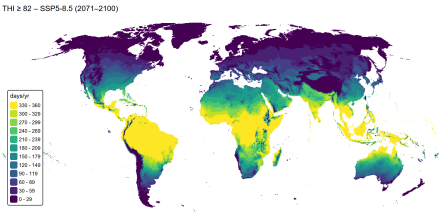

(f) THI $\geq$ 82 – SSP5–8.5

Figure 5: Sensitivity of projected heat-stress exposure to alternative THI thresholds. Each row compares the baseline period (left) with end-century projections under SSP5–8.5 (right) for thresholds of 68, 77 and 82.

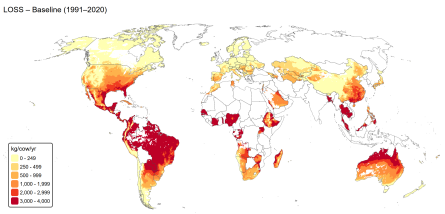

(a) Baseline (1991–2020)

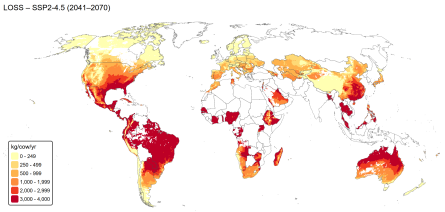

(b) SSP2–4.5 (2041–2070)

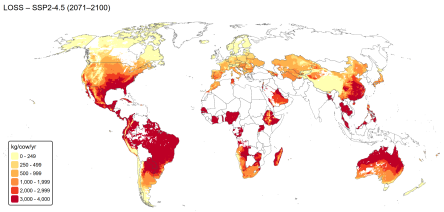

(c) SSP2–4.5 (2071–2100)

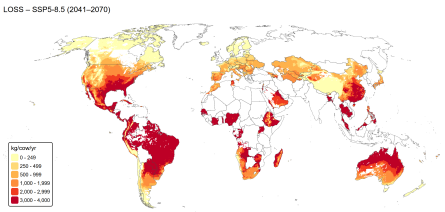

(d) SSP5–8.5 (2041–2070)

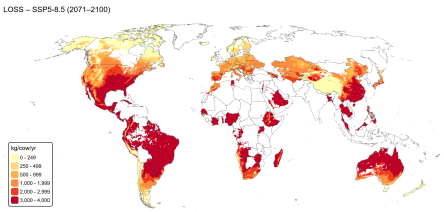

(e) SSP5–8.5 (2071–2100)

Figure 6: Ensemble-mean annual milk-yield loss per cow (kg cow^{-1} yr^{-1}) estimated from the quadratic St-Pierre function for the baseline (1991–2020) and mid- and end-century periods under SSP2–4.5 and SSP5–8.5. Results are shown for regions retained by the livestock mask.

Table 1: Annual milk-yield losses for OECD countries (baseline and end-century SSP5–8.5), and future losses per capita.Losses are aggregated over dairy cattle density (GLW3) using the St-Pierre heat-stress function applied to ensemble-mean THI. Per-capita values use FAO population (2010–2014).

Country	**$\text{Loss}_{\text{pres}}$ (Mt/yr)**	**Loss_{fut} (Mt/yr)**	**Loss_{fut} per inhabitant (kg/yr/inhab)**
Australia	46.97	102.81	4497.0
Austria	0.179	1.386	153.9
Belgium	0.275	1.667	144.4
Canada	2.399	14.523	372.2
Chile	0.411	1.775	88.0
Colombia	150.221	309.495	5829.7
Costa Rica	6.455	13.077	2558.9
Czechia	0.176	1.081	101.0
Denmark	0.034	0.293	50.4
Estonia	0.011	0.080	60.3
Finland	0.029	0.258	46.6
France	3.142	16.985	254.0
Germany	1.371	8.984	108.4
Hungary	0.337	1.335	135.7
Iceland	0.000	0.000	0.02
Ireland	0.016	0.523	104.2
Israel	0.645	1.629	171.8
Italy	2.388	10.765	177.3
Japan	1.654	5.574	44.4
Latvia	0.025	0.171	89.5
Lithuania	0.063	0.404	144.5
Luxembourg	0.027	0.145	229.3
Mexico	113.175	231.689	1808.1
New Zealand	0.173	2.198	445.0
Norway	0.006	0.075	13.9
Poland	0.785	4.391	115.5
Portugal	0.592	2.348	232.5
Slovakia	0.106	0.512	93.7
Slovenia	0.084	0.527	250.9
Spain	2.339	9.130	194.1
Sweden	0.053	0.426	41.3
Switzerland	0.079	0.766	85.9
United States	114.171	294.937	928.7